Brazilian Journal
of Chemical
Engineering

ISSN 0104-6632
Printed in Brazil
www.abeq.org.br/bjche

Vol. 26, No. 04, pp. 695 - 704, October - December, 2009

CAPILLARY HOLDUP BETWEEN VERTICAL SPHERES

S. Zeinali Heris[1*], M. T. Hamed Mosavian[1] and E. T. White[2]

[1]Chemical Engineering Department, Faculty of Engineering, Phone/Fax: + (98) (511) 8816840,
Ferdowsi University of Mashhad, Mashhad, Iran.
E-mail: hmosavian@gmail.com, E-mail: mosavian@um.ac.ir,
[*]E-mail: zeinali@ferdowsi.um.ac.ir
[2]Chemical Engineering Department, The University of Queensland, QLD 4072, Australia.

(Submitted: March 03, 2009 ; Revised: August 16, 2009 ; Accepted: August 27, 2009)

Abstract - The maximum volume of liquid bridge left between two vertically mounted spherical particles has been theoretically determined and experimentally measured. As the gravitational effect has not been neglected in the theoretical model, the liquid interface profile is nonsymmetrical around the X-axis. Symmetry in the interface profile only occurs when either the particle size ratio or the gravitational force becomes zero. In this paper, some equations are derived as a function of the spheres' sizes, gap width, liquid density, surface tension and body force (gravity/centrifugal) to estimate the maximum amount of liquid that can be held between the two solid spheres. Then a comparison is made between the result based on these equations and several experimental results.
Keyword: Capillary Liquid Holdup; Centrifuge; Drainage Bed; Particle; Hydrodynamics.

INTRODUCTION

Investigation of the maximum liquid holdup between particles is closely related to the liquid drainage in a packed bed or porous media. Therefore, it has diverse applications in different fields such as centrifugal separation (Swindells, 1982), sintering (Xu and Mehrabani, 1992), landfill saturation (Mcenroe, 1993), oil recovery from reservoirs (Owens and Ziegler, 1995; Luan and Ying, 1994; Espie, 1994) and airport and highway pavements (Casagrande and Shannon, 1951).

Phase holdup is an important hydrodynamic characteristic of multiphase systems relevant to optimization and scale-up of related process equipment. There are only few studies related to liquid holdup prediction theoretically, experimentally or numerically (Wang et al., 2006; Xio et al., 2000; De Andrade Lima, 2006; Yin et al., 2002; Muzen and Cassanello, 2005; Van Hasselt et al., 1999; Bruce et al., 2004; Inglezakis et al., 2001; Afreka et al., 2007; Gomez et al., 2000; Ayude et al., 2007; Iliuta et al., 2002; Lopes and Quinta-Ferreira, in press; Rathess and Kannan, 2004; Atta et al., 2007).

Wang et al. (2006) measured phase distribution of solid particles, and oil droplets were conducted in a lab-scale stirred tank by sample withdrawal under various operating conditions. An Eulerian-Eulerian three-fluid model was established for numerical simulation of a liquid-liquid-solid three-phase model and this model was used to compare the experimental results for liquid holdup with numerical model prediction.

Based on theoretical analysis and experimental results, Xiao et al. (2000) made new attempts to characterize the dynamics of the fluid flowing under conditions of pulsing flow in a trickle-bed reactor. They indicated that the proposed correlation could predict the dynamic holdup for a given packing type and given operating conditions. Based on a hydrodynamic study performed in a bench scale

[*]To whom correspondence should be addressed

column, Andrade Lima (2006) found that the dynamic saturation of the bed increases with the flow rate, while the static saturation decreases slightly.

Yin et al. (2002) measured the liquid (water) holdup distribution in a large scale packed column filled with metal pall rings using a gamma ray tomography technique. It was found that the liquid holdup distribution was not uniform and that the liquid distributor design had a significant effect on the holdup distribution. To simulate the liquid holdup distribution in a packed column, a set of volume averaged equations for the hydrodynamics was solved with the commercial computational fluid dynamics (CFD) software, CFX4.2. Simulation results were found to agree with the experimental data.

Muzen and Cassanello (2005) carried out an experimental study of the liquid holdup axial profile in a square section column with structured packing. Axial profiles of liquid holdup in the cocurrent and countercurrent operation were illustrated for liquid velocities below the loading point, and for solutions of different viscosity and foaming character. They indicated that variations between operation modes are larger for the foaming liquid than for the other liquid solutions employed.

Van Hasselt et al. (1999) measured liquid holdup as a function of gas and liquid mass flow in the three level of porosity (TLP) reactor. Packing materials and bed height were varied. Because a TLP reactor contains a layer of catalyst, there is an additional bed holdup compared to conventional trickle bed reactors. Liquid bed holdup was composed of two parts; below the capillary fill height, the interparticle pores are completely filled with liquid; above this height, the liquid holdup was well described by literature relations for single-phase trickle flow. Using residence time measurements, it was shown that no stagnant zones for liquid flow existed in the tested TLP packing. Bruce et al. (2004) collected experimental data on liquid holdup over a wide range of variables in a turbulent bed contactor with a 3mm projection of a gasket to block the free area of the distributor plate near the wall so that the channeling of liquid along the wall was avoided. The variation in dynamic liquid holdup based on static bed height with gas velocity, liquid velocity, particle diameter and density, static bed height, free-open area of the distributor plate and dimension of downcomer were discussed.

Inglezakis et al. (2001) proposed a simple tracing method, based on residence time distribution for the evaluation of the liquid holdup and dispersion in zeolite packed beds. Two tracers and two different materials, one porous and one non-porous, were used in experiments on seven packed beds of different dimension, operating under downflow or upflow conditions. The tracing techniques tested were reliable and applicable for the determination of liquid holdup and dispersion in clinoptilolite beds. An approximate correlation was proposed for liquid holdup and Peclet number in zeolite packed beds.

Afreka et al. (2007) determined static liquid holdup in a reactive distillation column packed with Katapak-SP12^{TM} elements, using a non-intrusive X-ray tomographic technique. X-ray tomography is probably the only experimental technique that is able to measure the distribution non-invasively on an operating column. Experiments were performed in a 10cm PVC column with the air-water system. The technique allows a local determination of the various liquid holdups as well as of the capillary height, without dismantling the elements.

Gomez et al. (2000) developed a new dimensionless correlation for the liquid holdup in the slug body. The correlation incorporates the mixture velocity, liquid viscosity, pipe diameter and inclination angle. The correlation was based on six up-to-date data sets. Ayude et al. (2007) explored temporal variation of the liquid holdup in a mini-pilot scale trickle bed reactor, induced by an ON-OFF liquid flow modulation strategy of operation at different axial positions. The effects of the liquid and gas superficial velocities, the bed depth and the cycling parameters, cycle period and split, on the liquid holdup modulation were examined for a wide range of conditions. For slow and intermediate cycle periods, the liquid holdup time dependence observed during the dry period was represented by an exponential function. The characteristic value of the decay was correlated with the examined variables.

Iliuta et al. (2002) provided a new mechanistic film model for the distribution of trickle-bed reactor hydrodynamic parameters (two-phase pressure drop, total external liquid holdup) in the low interaction regime. An important feature of the model is a more physical assumption of continuity in the velocity and shear stress profiles at the gas-liquid interface. This new approach has been successful in predicting the reactor hydraulics under various operational conditions such as atmospheric or high pressure/temperature conditions. Lopes and Quinta-Ferreira (in press) investigated the hydrodynamic behavior of a trickle-bed reactor at a high pressure in terms of pressure drop and liquid holdup after the development of a multiphase model by means of computational fluid dynamics (CFD) codes. The Eulerian multiphase model was then used in the

computation of pressure drop and liquid holdup and over a wide range for the calculated flow regime as a function of gas and liquid flow rates; the CFD theoretical predictions were in good agreement for both hydrodynamic parameters. Reactive distillation combines reaction with separation in a single column, thereby increasing conversion for equilibrium limited reactions, minimizing side reaction and saving on recycle and capital costs.

Rathess and Kannan (2004) developed a correlation for the dispersed phase liquid holdup based on the operating variables, equipment parameters and flow distribution parameters estimated from the flow pattern studies. The current study provides pressure drop and holdup data for KATAPAK-SP12 packing contained in a 100 mm diameter column.

Atta et al. (2007) presented a computational fluid dynamics (CFD) model based on the porous media concept to model the hydrodynamics of two-phase flow in trickle-bed reactors. The two-phase Eulerian model describing the flow domain as a porous region has been used to simulate the macroscale multiphase flow in trickle beds operating under trickle flow regime using FLUENT 6.2 software. It was shown that, while being relatively simple in structure, this CFD model is flexible and predictive for a large body of experimental data presented in the open literature.

Hence, considering its importance, there have been many attempts to study the liquid bridge formed between two particles. However, the main theme of the majority of them were the forces required to separate two particles adhered by a liquid bridge (Erle et al. 1971; Adamsand and Perchard, 1985; Briscoe and Adams, 1987; Coughlin et al., 1982; Cross and Picknett, 1963; Cross and Picknett, 1968; Fisher, 1926). The main assumption in all those papers was the neglect of the body force (gravitational/centrifugal) effect due to the small particle size. Therefore, they are not applicable in a separation process such as centrifugation where the body force plays an important rule. Moreover, the consideration of liquid bridge volume in previous studies (Simons et al., 1994; Smith et al., 1930; Kruyer, 1958; Mehrotra and Sastry, 1980; Mason and Clark, 1965; Rose, 1958; Melrose, 1966) was just the liquid holdup volume for the given filling angle and not the maximum liquid hold up at equilibrium.

For this study, consider a sphere of radius r_1 (Figure 1) that is vertically mounted below a second sphere of radius r_2, with a gap between the spheres of w. If the spheres are close enough, liquid can form a capillary ring of liquid between the two spheres. It is the purpose of this paper to estimate the maximum amount of liquid that can be held between the two spheres as a function of the spheres' sizes, gap width, liquid density, surface tension and body force (gravity/centrifugal).

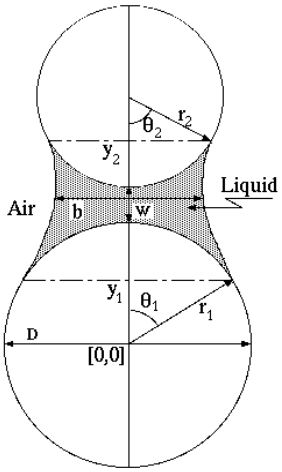

Figure 1: Liquid bridge between two particles

DERIVATION

The basic relation at a point in a static curved interface between two fluids is [Batchelor, 1974],

$$\Delta P = \sigma\left(\frac{1}{\kappa_1}+\frac{1}{\kappa_2}\right) \tag{1}$$

where ΔP is the pressure difference across the interface, where the curvatures of the surface are κ_1 and κ_2, and σ is the interfacial tension between the two fluids. For the case considered, vertical axisymmetry may be assumed. It will also be assumed that the interface curvature in the cylindrical direction is much larger than that normal to the cylinder and so the ring curvature κ_1 will be taken as constant. For cylindrical symmetry, it is only necessary to find the equation of the line that, by rotation, gives the interface surface. If the equation of this line is represented by y = y(x), then $1/\kappa_2 = y''/(1+y'^2)^{3/2}$, where $y' = dy/dx$ and $y'' = d^2y/dx^2$. The pressure difference across the interface, ΔP, will vary with height as $\Delta P = \Delta P_o + (\rho - \rho_a)gy$, where ρ and ρ_a are the densities of the liquid and gas and y is measured from a horizontal datum where the pressure

difference is ΔP_o. The basic relation (1) then becomes

$$\Delta P_o + (\rho - \rho_a) g y = \sigma \left(\frac{1}{\kappa_1} + \frac{y''}{(1+y'^2)^{3/2}} \right) \quad (2)$$

The y datum is taken as the vertical line joining the sphere centers, while the x datum is taken as the horizontal plane through the lower sphere center. The horizontal planes passing through the attachment of the liquid interface to the bottom and top spheres (point y_1 and y_2 in Figure 1) give rise to the following boundary conditions,
At point y_1:

$$\frac{x_1}{r_1} = \sin\theta_1 \quad (3)$$

$$y_1' = \tan\theta_1 = \frac{x_1 / r_1}{\left(1 - \left(\frac{x_1}{r_1}\right)^2\right)^{0.5}} \quad (4)$$

At point y_2:

$$\frac{x_2}{r_2} = \sin\theta_2 \quad (5)$$

$$y_2' = \tan\theta_2 = \frac{x_2 / r_2}{\left(1 - \left(\frac{x_2}{r_2}\right)^2\right)^{0.5}} \quad (6)$$

By non-dimensionalising the length variables with respect to the radius of the bottom sphere, i.e., $X = x / r_1$ and $Y = y / r_1$, the following dimensionless form of (2) is obtained:

$$\frac{Y''}{(1+Y'^2)^{3/2}} = \alpha Y + \beta \quad (7)$$

where

$$\alpha = \frac{(\rho - \rho_a) g r_1^2}{\sigma} = \frac{N_{cap}}{4} \quad (8)$$

and

$$\beta = \frac{r_1}{\kappa_1} + \frac{\Delta P_o r_1}{\sigma} \quad (9)$$

N_{cap} is the Capillary number $= (\rho - \rho_a) g D_1^2 / \sigma$, where D_1 is the diameter of the bottom sphere. For a given fluid and sphere diameter, κ_1 and ΔP_o are not known a priori and are dependent variables in the calculation, so that β is not an independent parameter.

The boundary condition equations (3-6) can also be non-dimensionalised (where $R = r_2 / r_1$) to arrive at the following expressions:

$$X_1 = \sin\theta_1 \quad (10)$$

$$Q_1 = Y_1' = \tan\theta_1 = \frac{X_1}{\left(1 - X_1^2\right)^{0.5}} \quad (11)$$

$$X_2 = R \sin\theta_2 \quad (12)$$

$$Q_2 = Y_2' = \tan\theta_2 = \frac{X_2}{\left(R^2 - X^2\right)^{0.5}} \quad (13)$$

Using $Y' = dY / dX = Q$, $Y'' = QdQ / dY$ allows (7) to be integrated to give:

$$-(1+Q^2)^{-0.5} = \left(\frac{\alpha}{2}\right) Y^2 + \beta Y + \gamma \quad (14)$$

In addition, substituting the boundary condition of (11) allows the integration constant γ to be evaluated as follows:

$$\gamma = -\cos\theta - \left(\frac{\alpha}{2}\right) Y_1^2 - \beta Y_1 \quad (15)$$

Therefore, by substituting equation (15) into (14), the following correlation can be obtained:

$$-(1+Q^2)^{0.5} = \left(\frac{\alpha}{2}\right)(Y - Y_1)^2 + \beta(Y - Y_1) - \cos\theta_1 \quad (16)$$

or

$$Q = Y' = \sqrt{\frac{1}{\left(\left(\frac{\alpha}{2}\right)(Y - Y_1)^2 + \beta(Y - Y_1) - \cos\theta_1\right)^2} - 1} \quad (17)$$

The integration of correlation (17) has the following form:

$$X - X_1 = \int_{Y_1}^{Y_2} \frac{dY}{\sqrt{\frac{1}{\left(\left(\frac{\alpha}{2}\right)(Y - Y_1)^2 + \beta(Y - Y_1) - \cos\theta_1\right)^2} - 1}} \quad (18)$$

Here

$$Y_1 = \cos\theta_1$$

and

$$Y_2 = R(1-\cos\theta_2) + W + 1$$

and

$$W = \frac{w}{r_1}$$

The volume of liquid V is then obtained by evaluating the volume of revolution

$$\frac{V}{\pi R_1^3} = -(1-\cos\theta_1)\frac{(2+\cos\theta_1-\cos^2\theta_1)}{3} - \frac{(1-\cos\theta_2)(2+\cos\theta_2-\cos^2\theta_2)}{3R^3} + \int_{Y_1}^{Y_2} X^2 dY \quad (19)$$

for $W > 0$

Method of Solution

Equation (18) cannot be solved analytically. Numerically, it can be solved by simple quadrature to give the interface profile (Y vs. X). However, numerical solution requires values of α, β and θ_1 before the solution can be found. But β and θ_1 are not known a priori. Thus, it is not possible to get a direct solution given the radii of the two spheres r_1, r_2, the gap w between them and the properties of the liquid.

It is a boundary value problem with the location of both boundary points unknown. An initial value solution method was chosen with inputs α, β and θ_1. The corresponding interface profile is calculated and the upper sphere radii R and gaps W which would give this interface are evaluated. Repeating this for wide ranges of α, β and θ_1 and interpolating allows solutions for any prescribed geometry.

For any point on the interface curve (X_2, Y_2), the corresponding upper sphere radius R and the gap width $W = w/r_1$ can be found by using the boundary conditions (equations 12 and 13) as,

$$\tan\theta_2 = Q_2 \qquad \text{(from (13))} \quad (20)$$

$$R = \frac{X_2}{\sin\theta_2} \quad (21)$$

$$W = Y_2 - R(1-\cos\theta_2) - 1 \quad (22)$$

If the solution is required for a known value of liquid property (α), particle size ratio (R) and the gap between the particles (W), the following steps are to be followed:

1. Choose a value for β and θ_1. Then, from (17), calculate Y' for all the points on the interface curve (X, Y).
2. Using equations 20, 21 and 22, calculate R and W for all the points on the interface curve (X, Y).
3. Plot R vs. W. If the line passes through the known values of R and W, then proceed to next step; otherwise, change the value of θ_1 and go back to step 2 until it does pass through.
4. Plot the interface(X, Y) and the particle boundary.
5. If the interface (X, Y) is just tangent to the solid particle boundary, then the value of β will be reduced and one will have to go back to step 2. This procedure is continued until the interface (X, Y) starts crossing the solid particles' boundary.
6. The value of β just before the intersection of the solid particles' boundary with the liquid bridge interface profile is the required solution.
7. Once the values of α, β, θ_1, R, and W are known, the values of interface(X, Y) and θ_2 can be calculated from (18).

Different Experimental Cases

1. Consider the case where the particles are of the same size with no gap between them, i.e., R = 1 and W = 0. Let $\alpha = 5$, $\theta_1 = 60$ and $\beta = -1$. Evaluating from (17) gives dY / dX as a function of Y (Figure 2).
2. Using the quadrate of (18) (i.e., integrating under the curve of Figure 2), the interface profile can be determined. Using equations 20-22, calculate θ_2, R and W for all the points on the interface (Figure 3). Negative values of W correspond to spheres with segments removed at the contact plane. (It really is of no concern what shape is hidden beneath the liquid. All that is required is that the surfaces are spherical at the line of contact with the liquid.) As the radius of the upper sphere $R \to \infty$, the solution should approach that of a sphere and a flat plate. Orr et al. (1975) have considered this case where the bodies are in contact.
3. Change the value of θ_1 to the new one, i.e., $\theta_1 = 65.66$, and go back to step 2. The new value of θ_1 complies with the required value of R and W (Figure 3).

4. The liquid bridge interface profile is shown in Figure 4 and is tangent to the solid particles boundary. Therefore, the value of β should be reduced. When β = -2, the required θ_1, which passes the requirement (i.e., R = 1, W = 0), is θ_1 = 81. But when the liquid interface is plotted, it crosses the solid particles' boundary. Therefore, the value of β has to be greater than -2.

5. For this specific case, the value of β = -1.

6. Knowing the value of α, β, θ_1, R and W, one can then go back to step 2 and calculate the interface profile (solid line in Figure 3).

The same technique has been used to calculate the liquid interface profile for a range of N_{cap} varying from 0 to 600. The result is shown in Figure 5. It is obvious from the results that, in the extreme case when $\alpha \rightarrow 0.0$, i.e., when either particle size $\rightarrow$ 0.0 or g $\rightarrow$ 0.0, the shape of the liquid bridge changes from concave to convex form and finally at α = 0.0, it is of a spherical shape.

Once the liquid bridge neck diameter is measured experimentally, its dimensionless volume can be calculated from the equation given in Table 1.

For a better understanding of the interface shape, the filling angles for the lower and upper particle (θ_1, θ_2) are given as a function of N_{cap} in Figure 6. The variation of parameters such as θ_1, θ_2, (b/D), $(V/(\pi R^3))$ and β with respect to N_{cap} is shown in Figure 6. Once the value of N_{cap} is known, these parameters can be evaluated by using the appropriate equation given in Table 1.

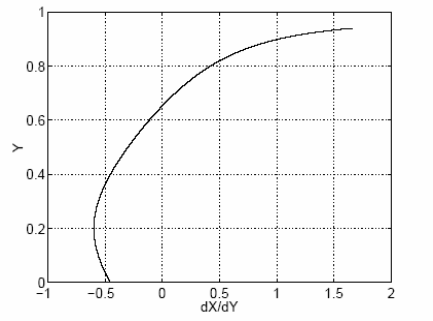

Figure 2: Liquid bridge interface's slope as a function of Y

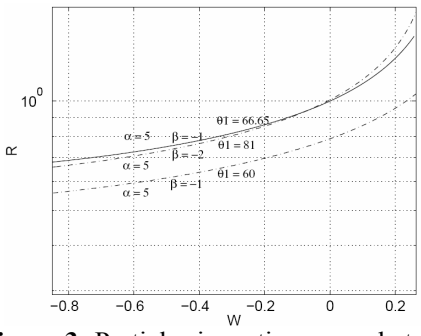

Figure 3: Particle size ratio vs. gap between two particles

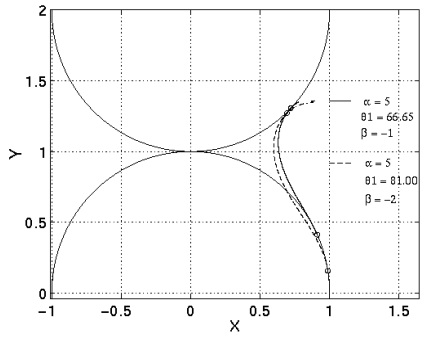

Figure 4: Liquid bridge between two equal size particles

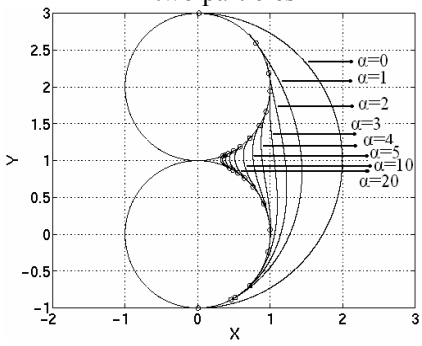

Figure 5: Liquid bridge profile calculated for values of α varying from zero to 150.

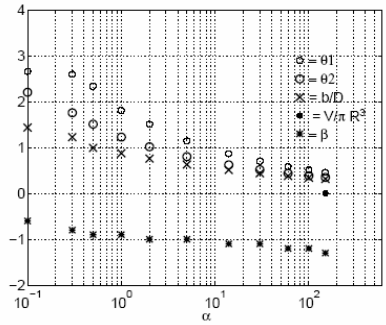

Figure 6: Different parameters as a function of N_{cap}

Table 1: Different parameters as a function of N_{cap}

Parameter	Equation	Constants
β	$\frac{1}{a + b\, N_{cap}^{0.5} + c\, e^{-N_{cap}}}$	a = –1.09179 b = 0.010640717 c = –0.91926777
$\frac{V}{\pi R^3}$	$a + \left(\frac{b}{1 + \left(\frac{N_{cap}}{c} \right)^d} \right)$	a = –0.013064384 b = 7.937831 c = 0.19149108 d = 0.88337687
θ_1	$a + \left(\frac{b}{1 + \left(\frac{N_{cap}}{c} \right)^d} \right)$	a = 0.43495617 b = 2.6853361 c = 5.252405 d = 0.76217257
θ_2	$a + \left(\frac{b}{1 + \left(\frac{N_{cap}}{c} \right)^d} \right)$	a = 0.30992848 b = 2.8383259 c = 1.2548094 d = 0.58595614
$\frac{b}{D}$	$a + \left(\frac{b}{1 + \left(\frac{N_{cap}}{c} \right)^d} \right)$	a = 0.28062047 b = 1.7237998 c = 1.394592 d = 0.54408581

EXPERIMENTAL SETUP

It involves two equal size glass spheres mounted vertically, one above the other. Saturating the surrounding air, the bottom tray is filled with the same liquid with which the experiment is carried out (Figure 7). Then the upper glass sphere is raised by a few mm. Using a syringe, the gap between the particles is overfilled with the liquid. Then the upper particle descends to contact the lower sphere. Using a traveling microscope, the neck diameter of the liquid bridge is recorded from time to time until it reaches a steady state. Each test was repeated 3 to 6 times and the uncertainty was lower than 10%, depending on the test. Also, the whole setup was kept in a cover (glass beaker) to maintain a saturation condition. However, the possibility of variation of temperature was unavailable.

The spherical particles considered for these experiments varied in size from 10 mm to 40 mm in diameter. The liquids used in the experiments were oil, water and four different dilutions of molasses. We have also tested different types of lower support and observed no effects on the liquid bridge neck diameter. One of the lower supports tested was a glass rod of about 2 mm diameter, which was fixed inside the glass ball itself.

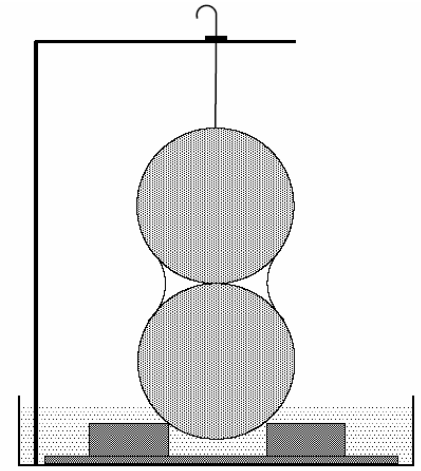

Figure 7: The experimental setup

RESULTS

Taking into account the shape of the liquid interface and also the amount of liquid trapped between two particles, the experimental results are presented in Figures 8 and 9. In Figure 8, b/D is the dimensionless liquid bridge neck diameter, which represents the shape of the liquid interface as a function of N_{cap}. The neck diameter is considered to be the minimum value of X for interfaces with a concave profile and the maximum value of X for a convex interface profile. These minima / maxima are measured only in the inner half region of the spheres.

First, we assume that the profiles of the liquid interfaces from the experimental results and the theoretical model are the same. Then we calculate the dimensionless liquid volume $(V/(\pi R^3))$ as a function of (b / D). The results (Figure 9) show good agreement.

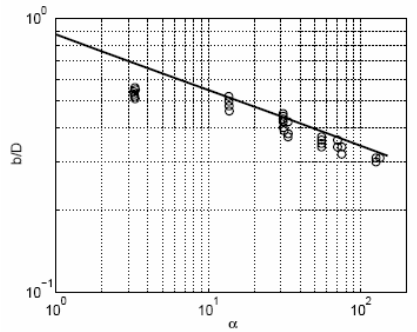

Figure 8: Liquid bridge neck diameter as a function of α

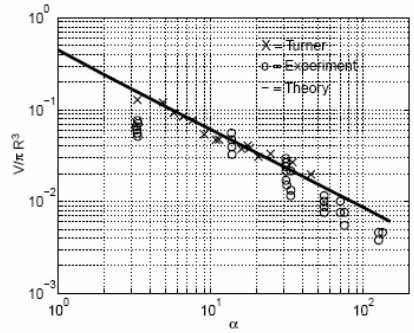

Figure 9: The comparison of experimental and theoretical value for dimensionless liquid bridge volume

CONCLUSIONS

Since it is believed that the static liquid holdup between the particles makes the major contribution towards carrying over impurities in the sugar crystal centrifugal separation process, this study has focused on capillary liquid holdup. In the present study, relevant equations are derived as functions of the sphere diameters, gap width, liquid density, surface tension and body force (gravity/centrifugal) to estimate the maximum amount of liquid that can be held between the two solid spheres. In addition, the gravitational effect was not neglected in the theoretical model. Comparison of results shows good agreement between derived correlations and experimental measurements.

NOMENCLATURE

a, b, c, d	Constants
b	Bridge neck diameter
D	Lower particle diameter
g	Gravity constant
r_1	Radius of the lower particle
r_2	Radius of the upper particle
R	Dimensionless radius (r_2 / r_1)
V	Volume
X_1	x_1 / r_1
X_2	x_2 / r_2
Y_1	y_1 / r_1
Y_2	y_2 / r_2
N_{cap}	Capillary number
w	Gap between particles
W	w / R
α	$\frac{N_{cap}}{4}$
β	The parameter defined in equation (9)
ΔP	Pressure difference across the interface
θ_1	Filling angle
θ_2	Upper filling angle
ρ	Liquid density
ρ_a	Air density
σ	Surface tension

REFERENCES

Adamsand M. J., Perchard, V., The cohesive forces between particles with interstitial liquid, Inst. Chem. Eng. Symp. Series 91, p. 147 (1985).

Aferka, S., Crien, M., Saroha, A. K., Toyo, D. and Marochot, P., In situ measurements of the static liquid holdup in Katapak-SP12™ packed column

X-ray tomography, Chemical Engineering Science 62, p. 6076 (2007).

Atta, A., Roy, S., Nigam, K. D. P., Prediction of pressure drop and liquid holdup in trickle bed reactor using relative permeability concept in CFD, Chemical Engineering Science 62, p. 5870 (2007).

Ayude, M. A., Martinez, O. M. and Cassanello, M. C., Modulation of liquid holdup along a trickle bed reactor with periodic operation, Chemical Engineering Science 62, p. 6002 (2007).

Batchelor, G. K., An introduction to fluid dynamics, Cambridge University Press (1974).

Briscoe, B. J. and Adams, M. J., Tribology in Particulate Tcnology, Bristol, UK IOP Publishing Ltd. (1987).

Bruce, A. F. R., Sai, P. S. T. and Krishnaiah, K., Liquid holdup in turbulent bed contactor, Chemical Engineering Journal, 99, p. 203 (2004).

Casagrande, A. and Shannon, W. L., Base course drainage for airport pavements, Proc. Amer. Soc. Civil Eng. 77, p. 1 (1951).

Coughlin, R. W., Elbirli, B. and Vergara-Edwards, L., Interparticle force conferred by capillary-condensed liquid at contact points, J. Colloid and Interface Sci. 87, p. 18 (1982).

Cross, N. L. and Picknett, R. G., Particle adhesion in the presence of a liquid film, Proc. Int. Conf. on Mechanisms of Corrosion by Fuel Impurities, p. 383 (1963).

Cross, N. L. and Picknett, R. G., Comment on the paper 'the effect of capillary liquid on the force of adhesion between spherical solid particles, J. Colloid and Interface Sci. 26, 247-249 (1968).

De Andrade Lima, L. R. P., Liquid Axial dispersion and holdup in column leaching, Minerals Eng. 19, p. 37 (2006).

Erle, M. A., Dyson, D. C. and Morrow, N. R., Liquid bridges between cylinders, in a torus, and between spheres, AICHE, Journal 17, p. 115 (1971).

Espie, A. A., A laboratory investigation of gravity drainage/water flood interaction in Prudhoe Bay, Society of Petroleum Engineers 28614, p. 47 (1994).

Fisher, R. A., On the capillary forces in an ideal soil; correction of formulae given by W.B. Haines, J. Agric. Sci. 16, p. 492 (1926).

Gomez, L. E., Shoham, O. and Taitel, Y., Prediction of slug liquid holdup: horizontal to upward vertical flow, International Journal of Multiphase Flow 26, p. 517 (2000).

Iliuta, I., Grandjean, B. P. A. and Larchi, F., New mechanistic film model for pressure drop and liquid holdup in trickle flow reactors, Chemical Engineering Science 57, p. 3359 (2002).

Inglezakis, V. J., Lemonidou, M. and Grigoropoulou, H. P., Liquid holdup and flow dispersion in zeolite packed bed, Chemical Engineering Science, 56, p. 5049 (2001).

Kruyer, S., The penetration of mercury and capillary condensation in packed spheres, Trans. Faraday Soc., 54, p. 1758 (1958).

Lopes, R. J. G. and Quinta-Ferreira, R. M., Three-dimensional numerical simulation of pressure drop and liquid holdup for high-pressure trickle-bed reactor, Chemical Engineering Journal, Article in Press.

Luan, Z. and Ying, D., Some theoretical aspect of gravity drainage in naturally fractured reservoirs, Society of Petroleum Engineers 28641, p. 357 (1994).

Mason, G. and Clark, W. C., Liquid bridges between spheres, Chem. Eng. Sci., 20, 859-866 (1965).

Mcenroe, B. M., Maximum saturated depth over landfill liner, J. Environ. Eng. 19, p. 262 (1993).

Mehrotra, V. P. and Sastry, K. V. S., Pendular bond strength between unequal-sized spherical particles, Powder Technology 25, p. 203 (1980).

Melrose, J. C., Model calculations for capillary condensation, AIChE Journal 12, 986-994 (1966).

Muzen, A. and Cassanello, M. C., Liquid holdup in columns packed with structured packing: Countercurrent vs. cocurrent operation, Chemical Engineering Science 60, p. 6226 (2005).

Orr, F. M., Scriven, L. E. and Rivas, A. P., Pendular ring between solids: Meniscus properties and capillary force, J. Fluid Mech. 67, p. 723 (1975).

Owens, B. K. and Ziegler, V. M., An oil production model for a well producing by both gravity drainage and viscous flow from a mature steamflood, Society of Petroleum Engineers 29656, p. 409 (1995).

Ratheesh S., and Kannan, A., Holdup and pressure drop studies in structured packings with catalysts, Chemical Engineering Journal 104, p. 45 (2004).

Rose, W., Volumes and surface areas of pendular rings, J. Appl. Phys. 29, p. 687 (1958).

Simons, S. J., Seville, J. P. K. and Adams, M. J., An analysis of the rupture energy of pendular liquid bridges, Chem. Eng. Sci. 49, p. 2331 (1994).

Smith, W. O., Foote, P. D. and Busang, P. F., Capillary retention of liquids in assemblages of homogeneous spheres, Phys. Rev. 36, p. 524 (1930).

Swindells, R. J., A mathematical model of a continuous sugar centrifuge, in PhD thesis, Chemical Engineering Department., The University of Queensland: Australia (1982).

Van Hasselt, B. W., Calis, H. P. A., Sie, S. T. and van den Bleek, C. M., Liquid holdup in the three-

level-of-porosity reactor, Chemical Engineering Science 54, p. 1405 (1999).

Wang, F., Mao, Z. S., Wang, Y. and Yang, C., Measurment of phase holdups in liquid-liquid-solid three phase stirred tanks and CFD simulation, Chem. Eng. Sci. 61, p. 7535 (2006).

Xio, Q., Anter, A. M., Cheng, Z. M. and Yuan, W. K., Correlation for dynamic liquid holdup under pulsing flow in a trickle-bed reactor, Chem. Eng. J. 78, p. 125 (2000).

Xu, K. and Mehrabadi, M. M., On the liquid bridge profile and capillary forces in the initial stage of sintering, ASME MD 37, p. 115 (1992).

Yin, F., Afacan, A., Nandakumar, K., Chuang, K. T., Liquid holdup distribution in packed columns: gamma ray tomography and CFD simulation, Chemical Engineering and Processing, 41, p. 473 (2002).